

Automated Kidney Detection and Segmentation in 3D Ultrasound

Matthias Noll^(✉), Xin Li, and Stefan Wesarg

Cognitive Computing and Medical Imaging, Fraunhofer IGD,
Fraunhoferstr. 5, Darmstadt, Germany
{matthias.noll,li.xin,stefan.wesarg}@igd.fraunhofer.de
[http://www.igd.fraunhofer.de/en/Institut/Abteilungen/
Cognitive-Computing-Medical-Imaging](http://www.igd.fraunhofer.de/en/Institut/Abteilungen/Cognitive-Computing-Medical-Imaging)

Abstract. Ultrasound provides the physical capabilities for a fast and save disease diagnosis in various medical scenarios including renal exams and patient trauma assessment. However, the experience of the ultrasound operator is the key element in performing ultrasound diagnosis. Thus, we like to introduce our automatic kidney detection and segmentation algorithm for 3D ultrasound. The approach utilizes basic kidney shape information to detect the kidney position. Following, the Level Set algorithm is applied to segment the detection result. In combination this method may help physicians and inexperienced trainees to achieve kidney detection and segmentation for diagnostic purposes.

Keywords: Ultrasound · Image analysis · Kidney · Shape prior · Detection · Segmentation

1 Introduction

Ultrasound is a widespread medical imaging system that provides a fast, non-invasive and non-hazardous way to obtain patient anatomy information. Despite its importance in medicine there are some challenges that have to be addressed when dealing with ultrasound images. Speckle, artifacts and generally a poor signal-to-noise ratio highly influence the image quality [7] and are therefore the hardest challenges to overcome. Additionally, the specific ultrasound intensity values fluctuate between consecutive recordings and vary even strongly between miscellaneous ultrasound devices. Thus, physicians or medical technicians are given multiple ways to manipulate the imaging output to their individual preferences. All these factors have to be addressed when designing automatic ultrasound image analysis algorithms.

Currently, most ultrasound diagnosis are still performed using 2D ultrasound technology. This is because physicians are accustomed to the standard ultrasound modality. If 3D ultrasound is available, it is often only used to acquire patient recordings for later review. All 3D datasets including CT and MRI are commonly presented using cross section views with sliced volume information,



Fig. 1. eFAST recording of the right kidney. The image also includes the liver, the hepatorenal recess and a rib shadow extension (right).

which is hard to apply and work with in a live imaging systems like ultrasound [1]. A computer algorithm however can work directly on the 3D data.

The goal of this study was to design an automated kidney detection and segmentation method that utilizes the more and more available 3D ultrasound capability of ultrasound devices. The kidney is the target structure in this study, because it is frequently examined using ultrasound. Also, it has a unique bean-shape structure that is reasonably well recognizable by the human eye.

The kidneys are retroperitoneal organs that are protected by the lower ribs. Depending which kidney is the examination target, a recording is performed by placing the ultrasound transducer between the 5th to 9th intercostal space. During the exam the ultrasonographer must adhere the ribs, because they cause large shadow artifacts in the ultrasound that cannot be compensated during image processing. The right kidney is located just below the liver (see Fig. 1). Similar, the left kidney lies just below the spleen. Each kidney has a tough fibrous outer cortex that appears dark in the ultrasound. The inner renal sinus containing the renal pelvis with larger blood vessels, lymphatics and fatty tissue generates a brighter ultrasound echo, giving a good contrast to the outer cortex. Detecting and segmenting the kidney in ultrasound images could help in automating medical examination protocols like renal exams and eFAST. Also, this could help in creating an automated abdominal ultrasound diagnostic system.

2 Image Processing

2.1 Data Preparation and Pre-processing

Addressing the challenges mentioned in the introduction and generally enhance algorithm reproducibility, the influence of the image quality to the detection and segmentation is reduced [3]. We apply a multi-scale image pyramid (Fig. 2(a)) to the ultrasound, thereby reducing speckle and smoothing the image while preserving important larger abdominal structures [10]. Additionally, we adjust the

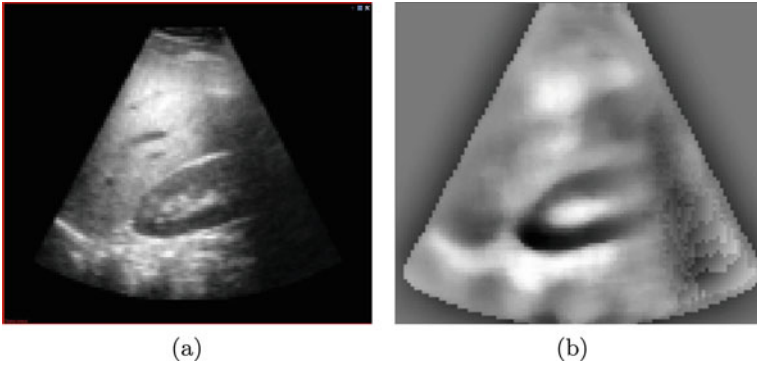


Fig. 2. (a) Downscaling of the input image. (b) Histogram equalized image with distinctive kidney shape

global image contrast through histogram equalization [8] (cf. Fig. 2(b)). This step is very time consuming and should be replaced with a more efficient alternative. We apply histogram equalization to decrease the image intensity fluctuations between different ultrasound recordings. For a kidney recording, the equalization result will usually contain the distinctive kidney shape composed of low intensity values.

After pre-processing we assume a bi-modal histogram composition for the equalization result. Applying Otsu’s method to the equalized image calculates the optimum image threshold by minimizing the intra-class variance, thereby automatically reducing the gray level intensity image to a binary representation [6]. As a result, we obtain a “kidney candidate image” (Fig. 3), containing all possible kidney locations. The dark kidneys outer cortex is represented with a binary *one*, while the inner sinus receives a binary *zero* value.

We generalize the algorithm further, by applying additional information about the segmentation target e.g. the kidney shape. Here, we chose a 3D ellipsoid structure element, that represents a rough shape approximation of the kidneys inner sinus (Fig. 4). The structure element size is $20 \times 10 \times 10$ mm, so it



Fig. 3. Kidney candidate image showing the kidney location with the kidneys outer cortex (red) and inner sinus (black). Also visible on the right a recorded rib shadow creating a candidate artifact (Color figure online).

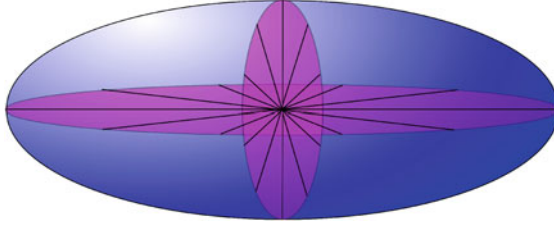


Fig. 4. Kidney structure element (shape prior). For simplicity the emitted rays (black) are illustrated for just two image directions.

will fit inside the kidney and especially inside the average renal pelvis. This is beneficial for the graph based search that is performed in the kidney detection step described in the next section. After the “structure element” selection we are able to utilize both signal and shape information during the image analysis. Advancing the algorithm in future implementations the simple structure element can be substituted by e.g. a model of the kidney sinus to gain specific shape information [9].

2.2 Detection

After the image pre-processing the kidney location is identified as follows. Initially, a search graph is constructed and applied to the kidney candidate image (Fig. 5(a)). The inter graph node step size is derived from the structure elements extent. The kidney structure element is then placed at each graph node. This way all possible kidney locations are investigated. In each step the structure element emits radial rays to each of the three image coordinate planes (see Fig. 5(b)). For a travel distance of $1.5\times$ the structure elements diameter in emission direction and using m discrete detection steps, each emitted ray r_j ascertains the presence of zero-one crossings in the binary kidney candidate image. Here, we

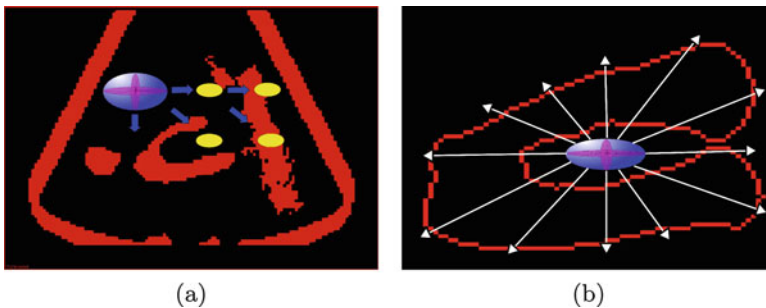


Fig. 5. (a) Graph-based searching using the kidney shape element on the kidney candidate image. (b) Detection of zero-crossings at the kidney position illustrated for the xy -image axis

utilize the differences in echogenicity between the inner and outer kidney fiber structures to detect the crossing from the renal pelvis to the outer cortex. Using the chosen structure element and the eFAST acquisition protocol, slight kidney rotations can be neglected. Strong rotations however will require an initial volume alignment. Each ray r_j with a detected zero-one crossing receives a ray score $f(i, j) = 1$, whereas the remaining rays receive a score of $f(i, j) = 0$. The kidney candidate with a score

$$S_c = \frac{\sum_{\substack{1 < i \leq n \\ 1 < j \leq n}} f(i, j)}{n}, f(i, j) \in [0, 1] \quad (1)$$

of 80 % or more corresponds to the kidney position (cf. Fig. 6). A candidate score $S_c < 80\%$ lead in some of the available test data to a false kidney detection at the ultrasound boundary. The score threshold parameter might be ultrasound device related and might need adjustment for other devices. Our tests showed further, that a number of $n = 12$ rays per image coordinate plane is sufficient to successfully detect the kidney location. Using more rays is always possible but ultimately will increase algorithm computation time. The candidate score would need adjustment. For recordings containing a rib shadow, using less than 12 rays lead to a false kidney detection. If more than one candidate achieves a score of 80 % or more, the candidate with the highest valid ray count is selected as the valid kidney position. Hence, the presented detection method will generate at most one kidney position. A successful graph search directly triggers the automated segmentation on the detection result.

2.3 Segmentation

For the remaining kidney candidate, each valid ray generates a seed point for the kidney segmentation. Here, the seed points are placed with an offset d to the detected crossing point along the rays direction. The offset d was chosen to be approximately half the diameter of the kidneys outer cortex. Following, the fast marching algorithm [4] is applied to the collection of seed points to generate an intermediate kidney segmentation. The fast marching algorithm is a basic segmentation algorithm that uses a constant segmentation propagation speed and predefined iteration steps. It also requires a speed function to restrict the

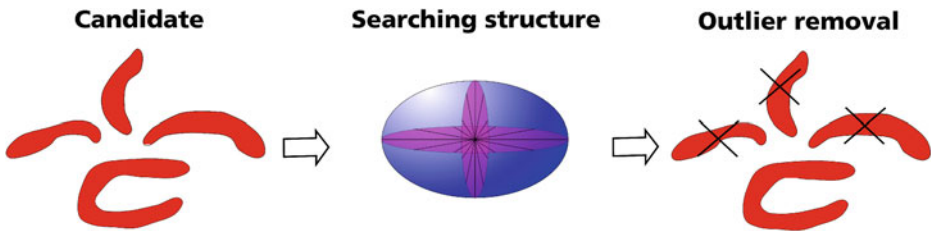


Fig. 6. Candidate search removes all invalid kidney candidates.

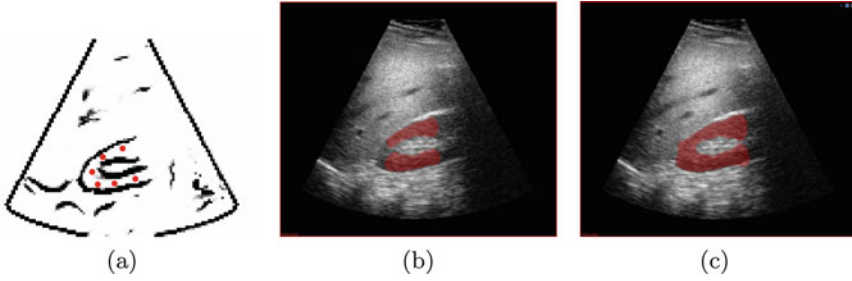


Fig. 7. Figure (a) shows the utilized speed function image (sigmoid) with indicated seed point placements. Figure (b) shows the intermediate segmentation result of the fast marching algorithm. The final segmentation result (b) was achieved by applying the Level Set algorithm.

segmentation propagation. We utilized a sigmoid computation of the histogram equalized input as the speed function (see Fig. 7(a)).

Because of this, the segmentation results are not always connected for all seed point areas (Fig. 7(b)). To achieve full segmentation connectivity we additionally apply the Level Set algorithm [2] to the intermediate fast marching segmentation result. The sigmoid image is once again used as the restricting speed function. The Level Set algorithm improved the segmentation result for most of the available test cases by connecting separated areas (cf. Fig. 7(c)). The output of the Level Set algorithm is the final segmentation result.

3 Results

We performed our experiments on 62 three-dimensional ultrasound data sets of 8 healthy male and female volunteers. The images were acquired using the right upper quadrant view of the eFAST exam. The kidney detection rate on the available data was above 90%. The kidney could not be automatically detected in six data sets due to strong rib shadows, that cut through the kidney location. Here, no kidney candidate achieved the necessary 80% valid rays criterion, because the shadow area included a large amount of image information about the inner kidney structure. The connection of kidney candidates to shadow artifacts (see Fig. 3) did not influence the detection result in the available test cases. However, avoiding rib shadows is still the most important task in acquiring data for the presented method. Due to this, we also implemented a shadow detection algorithm based on [5] to indicate the viability of an ultrasound recording for kidney detection.

The segmentation method was applied to the remaining 56 data sets, after the kidney detection generated a valid candidate. Some of the results are shown in (Fig. 8). However, the segmentation algorithm currently does not work properly in all of the available cases. In some images the Level Set leaked the kidney because of weak boundary gradients at the kidneys renal capsule. Here, the

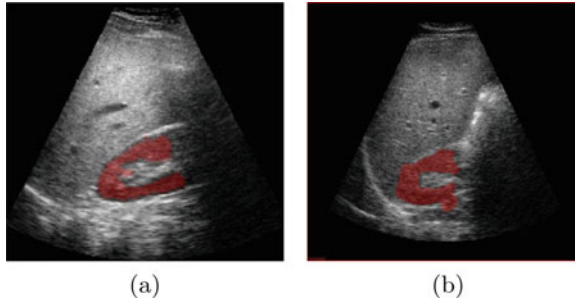


Fig. 8. Two example results of the proposed automated detection and segmentation method. In figure (b) a minor segmentation leak can be observed.

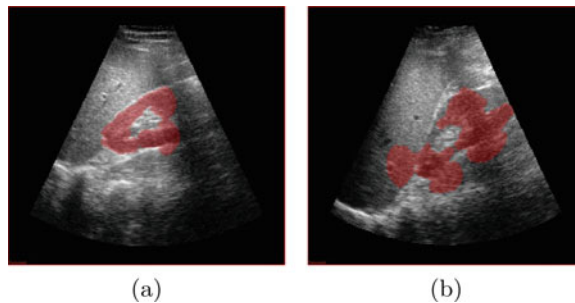


Fig. 9. Leaking Level Set results. Most commonly a leaking occurs at the threshold of a rib shadow (a). Figure (b) shows the worst leakage example of all 62 test data sets.

applied speed function did not generate the necessary restriction parameters to keep the algorithm from propagating the segmentation to the liver and other surrounding tissue. In (Fig. 9) we can see examples of the Level Set leaking the kidney with (Fig. 9(b)) being the worst result we achieved using the presented segmentation approach. Overall we are satisfied with the so far achieved results and we will continue working to improve the segmentation algorithm.

4 Conclusion

A method for automated kidney detection and segmentation in 3D ultrasound has been proposed. Both ultrasound image intensities and kidney shape priors in form of a structure element have been used in the process. The automated kidney detection was possible in all available data sets with no rib shadows. The kidney segmentation based on the detection results is feasible but has to be improved using more sophisticated algorithms before automatic diagnosis based on the segmentation result is achievable. We also believe, that the presence of a kidney can be excluded, if the number candidate score S_c does not exceed a certain threshold. We will investigate this possibility in further experiments

with a greater variety of test data sets. We further need to investigate kidney pathologies because the assumption of finding the bright inner sinus versus the dark outer cortex might not hold.

References

1. Aliakseyeu, D., Subramanian, S., Martens, J.B., Rauterberg, M.: Interaction techniques for navigation through and manipulation of 2d and 3d data. In: Proceedings of the Workshop on Virtual Environments, EGVE '02, pp. 179–188. Eurographics Association, Aire-la-Ville, Switzerland, Switzerland (2002)
2. Chen, T.F.: Medical Image Segmentation Using Level Sets, pp. 1–8 (2008)
3. Contreras Ortiz, S.H., Chiu, T., Fox, M.D.: Ultrasound image enhancement: a review. *Biomed. Signal Process. Control* **7**(5), 419–428 (2012)
4. Forcadel, N., Guyader, C., Gout, C.: Generalized fast marching method: applications to image segmentation **48**(1–3), 189–211 (2008)
5. Hellier, P., Coupe, P., Meyer, P., Morandi, X., Collins, D.: Acoustic shadows detection, application to accurate reconstruction of 3d intraoperative ultrasound. In: 5th IEEE International Symposium on Biomedical Imaging: From Nano to Macro, ISBI 2008, pp. 1569–1572 (2008)
6. Hirasakolwong, N., Hua, K.A., Vu, K., Windyga, P.S.: Segmentation of ultrasound liver images: an automatic approach. In: Proceedings of the 2003 International Conference on Multimedia and Expo - ICME '03, vol. 2, pp. 573–576. IEEE Computer Society, Washington, DC (2003)
7. Loizou, C., Pattichis, C., Istepanian, R., Pantziaris, M., Kyriakou, E., Tyllis, T., Nicolaides, A.: Ultrasound image quality evaluation. In: 4th International IEEE EMBS Special Topic Conference on Information Technology Applications in Biomedicine, pp. 138–141 (2003)
8. Peng, B., Wang, Y., Yang, X.: A multiscale morphological approach to local contrast enhancement for ultrasound images. In: Proceedings of the 2010 International Conference on Computational and Information Sciences, ICCIS '10, pp. 1142–1145. IEEE Computer Society, Washington, DC (2010).
9. Xie, J., Jiang, Y., Tsui, H.T.: Segmentation of kidney from ultrasound images based on texture and shape priors. *IEEE Trans. Med. Imag.* **24**(1), 45–57 (2005)
10. Zong, X., Laine, A.F., Geiser, E.A.: Speckle reduction and contrast enhancement of echocardiograms via multiscale nonlinear processing. *IEEE Trans. Med. Imag.* **17**(4), 532–540 (1998)